An Enhanced Model Predictive Control Strategy to Drive PMSM with reduced Torque and Flux Ripples

Masoud Nikbakht
Electrical engineering department
K. N. Toosi University of Technology
Tehran, Iran
MasoudNikbakht@email.kntu.ac.ir

Sahand Ghaseminejad Liasi
Electrical engineering department
K. N. Toosi University of Technology
Tehran, Iran
Ghaseminejad@ee.kntu.ac.ir

Karim Abbaszadeh
Electrical engineering department
K. N. Toosi University of Technology
Tehran, Iran
Abbaszadeh@eetd.kntu.ac.ir

Gholamreza Arab Markadeh
Electrical engineering department
Shahrekord University
Shahrekord, Iran
Arab-gh@eng.sku.ac.ir

***Abstract*— PMSMs are mainly controlled using DTC and FOC. However, these methods suffer from relatively high torque and stator flux ripples. This article proposes a model-predictive control strategy in which, exploiting stator flux observer and optimized cost function, the dynamic response of the motor is improved. The stator flux and y-axis current are considered as the state variables. Stator flux observer is used to estimate the flux and torque angles. Moreover, a cost function with optimized coefficients are used to optimize the model. A simulation in MATLAB/Simulink is carried out and the results are brought in the section V. The results show that the proposed control strategy decreases the torque and stator flux ripples by over 50%. Furthermore, the stator current THD has decreased over 30%.**

Keywords—PMSM, predictive-model control, hybrid control, torque ripple, flux ripple.

I. INTRODUCTION

Because of high power density, high efficiency and wide speed range of permanent magnet synchronous motors (PMSMs), they have been increasingly used in various applications including electric pumps, fans and electric vehicles [1,2].

PMSMs are mainly controlled using direct torque control (DTC) and vector control (VC), also known as field oriented control (FOC) [3,4]. Although these methods have some similarities, VC and DTC differ in practical implementation and mathematical modeling. While general VC is based on current control and has a smooth performance, general DTC enjoys a simpler implementation, faster dynamics and less dependence on parameter variations. Moreover, DTC offers decent torque control in both transient and steady state. However, DTC suffers from high flux and torque ripple.

Combined control methods are proposed based on the characteristics of these methods [6-8]. These methods have also been applied to linear induction motors and DFIGs [9], [10]. These methods enjoy the advantages of the two conventional methods in a way that the torque and flux ripple are less than DTC method and the transient dynamics and their steady state error are better than the VC method.

In [6], a hybrid approach is proposed in which the reference current values are calculated from the reference values of the flux and torque. In [7], a hybrid control method is offered, which uses hysteresis controller and PI flux controller. Authors in [8] have exploited a deviation model using switching table and hysteresis controller. Because of eliminating the PI controller, this method enjoys less dependency to the system parameters, which can be considered as an advantage. However, due to the use of hysteresis controller, flux and torque ripples, as well as switching frequency, are highly dependent on the hysteresis bandwidth.

Recently, model predictive control (MPC), due to its simplicity and the ability to consider nonlinear system parameters into the predicted model and calculate the behavior of variables for different switching modes, has been employed as an attractive and powerful method in power electronics. Therefore, MPC has been widely used in controlling multilevel inverters [11], Z-Source converters [12] and electric motor drives [13-15].

Finite control set MPC (FCS-MPC) is the most popular MPC method. In this method, according to the discrete converter or drive model, the system behavior is predicted for different switching modes and accordingly, the optimal switching vector, which minimizes the cost function, will be applied. A pragmatic comparison between predictive current control (PCC) and predictive torque control (PTC) is presented in [16]. The authors concluded that both of these methods have similar transient behavior, although PTC has less torque ripple than PCC. A robust current predictive control is presented in [17], where a prediction error constraint is added to the cost function. In [18], the reduction of torque ripple in the PTC is carried out by a slight change in the cost function. Adding switching frequency constraint to the PTC cost function, in [19], the reduction of switching frequency is performed, which has resulted in the reduction of inverter losses.

However, since all abovementioned strategies are founded on DTC, they suffer from relatively high torque ripple. This ripple leads to undesired mechanical tensions and increment of power loss, which decreases the system efficiency. In this vein, direct flux vector control (DFVC) can be considered as an alternative controller, which results in less torque ripples [20, 21]. DFVC uses PI controllers, which need to be tuned separately. To avoid exhausting PI tuning, a model predictive control (MPC) approach is used in this article. Simulation results validate the advantages of the proposed method over DTC and PTC methods.

In the following, first, AC machine model in the field-oriented frame will be explained. Then, predictive control will be discussed in section III and based on the provided formulation, the proposed method will be explained. Finally, a comparison between the proposed method with DTC and PTC will be carried out to prove the efficiency of the proposed method.

II. MOTOR MODEL IN THE FIELD-ORIENTED FRAME

The dynamic behavior of PMSM can be explained in terms of space vectors in various reference frames.

The DFVC method, presented in [20] and [21], is briefly described in this section. The reference axes of the rotor and the stator flux are presented in Fig. 1. Where (x-y) and (d-q) represent the stator flux reference and the rotor reference frame, respectively.

A. Ipmsm Model in Rotor Reference Frame

The interior PMSM (IPMSM) model in the rotor reference Frame are described by:

$$u_d = R_s i_d + \frac{d\lambda_d}{dt} - w\lambda_q \tag{1}$$

$$u_q = R_s i_q + \frac{d\lambda_q}{dt} + w\lambda_d \tag{2}$$

$$\lambda_d = L_d i_d + \lambda_m \tag{3}$$

$$\lambda_q = L_q i_q \tag{4}$$

u_d , u_q , i_d , i_q , λ_d , λ_q are d_q axis stator voltages, currents and fluxes respectively. R_s is the stator winding resistance and λ_m is the permanent magnet flux. w is the electrical rotor speed and L_d, L_q are the d-axis and q-axis inductances respectively.

The electromagnetic torque equations can be defined as:

$$T_e = \left(\frac{3}{2}\right) p\left(\lambda_m i_q + \left(L_d - L_q\right) i_d i_q\right) = \left(\frac{3}{2}\right) p\left(\lambda_d i_q - \lambda_q i_d\right) \tag{5}$$

Where p is the number of pole pairs.

B. IPMSM Model in Stator Flux Reference frame:

The IPMSM voltage equations in the stator flux reference frame are given by [1]:

$$u_x = R_s i_x + \frac{d\lambda_x}{dt} - (w + \frac{d\delta}{dt})\lambda_y \tag{6}$$

$$u_y = R_s i_y + \frac{d\lambda_y}{dt} + (w + \frac{d\delta}{dt})\lambda_x \tag{7}$$

Where u_x, u_y, i_x, i_y, λ_x, λ_y are x_y axis stator voltages, currents and fluxes, respectively. w_s is the stator flux electrical angular speed.

$$w + \frac{d\delta}{dt} = w_s \tag{8}$$

Where δ is the angle between stator flux and rotor frame that called load angle, defined in fig. 1. Of course, in steady-state conditions $w_s = w$.

Since in the selected reference frame $\lambda_y = 0$, (6) and (7) can be abridged as:

$$u_x = R_s i_x + \frac{d\lambda_x}{dt} \tag{9}$$

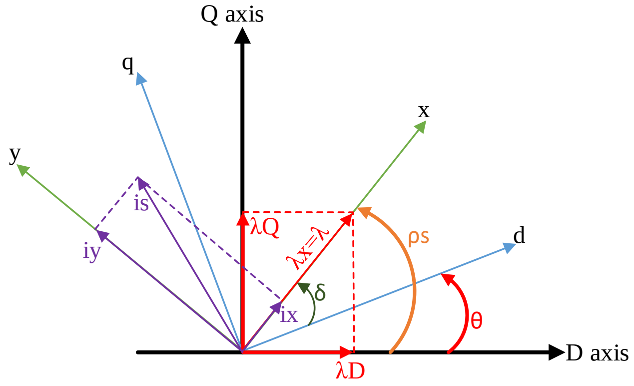

Fig. 1. Coordinates of IPMSM

$$u_y = R_s i_y + (w + \frac{d\delta}{dt})\lambda_x \tag{10}$$

In addition, the electromagnetic torque can be expressed as a function of the load angle by:

$$T_e = \frac{(\frac{3}{2})p}{Ld}\left[\frac{Ld-Lq}{Lq}\lambda^2 \frac{\sin 2\delta}{2} + \lambda_m \lambda.\sin\delta\right] \tag{11}$$

Obviously, both δ and λ are influential on the torque. Moreover, for a constant flux, the torque is adjusted by δ. However, the mentioned torque relationship is nonlinear and dependent on the model. Therefore, an alternative direct torque control method is suggested as follows:

$$T_e = \left(\frac{3}{2}\right) p\lambda i_y \tag{12}$$

Where λ is the stator flux amplitude. The torque producing current i_y defined in (12) is closed loop regulated on behalf of δ for the sake of torque control [20].

C. State Variables of DFVC

Since, in the DFVC method, the stator flux is controlled directly, the control method have to be based on the stator flux reference frame. The machine model has been presented in the stator flux reference frame in the previous section. This section, first, presents the DFVC state equations, then, selecting the appropriate state equations, the corresponding predictive control method will be presented. The flux and load angle observer is also presented.

According to (9) and (10), the state variables will be $\lambda_x = \lambda$, δ. The following relationships can be established.

$$\begin{bmatrix} \frac{d\delta}{dt} \\ \frac{d\lambda}{dt} \end{bmatrix} = \begin{bmatrix} 0 & 0 \\ 0 & 0 \end{bmatrix} \begin{bmatrix} \delta \\ \lambda \end{bmatrix} + \begin{bmatrix} \frac{u_y - R_s i_y}{\lambda} - w \\ u_x - R_s i_x \end{bmatrix} \tag{13}$$

In [22], a direct control of the stator flux and the load angle (torque angle) is presented. The state variables are the same as the variables selected in (13). It is worth to mention that the torque equation would be very complex in terms of δ and λ, which makes it impossible to obtain a linear relationship by controlling δ and λ. Therefore, instead of using δ, i_y, which results in torque generation, is selected as the second state variable. In this case, according to (9) and (10), the machine voltage equations in the stator flux reference frame changes as follows.

$$\frac{d\lambda}{dt} = u_x - R_s i_x \tag{14}$$

$$\frac{di_y}{dt} = -\frac{a}{L_d}(u_x - R_s i_x) + \frac{b}{L_d}(u_y - R_s i_y - w\lambda) \tag{15}$$

Where a and b are variables that are a function of the magnetic state of the machine and are defined as follows.

$$a(\delta) = \frac{1}{2}(1 - \frac{L_d}{L_q}) \sin 2\delta \tag{16}$$

$$b(\lambda, \delta) = -\left(1 - \frac{L_d}{L_q}\right) \cos 2\delta + \frac{\lambda_m}{\lambda} \cos\delta \tag{17}$$

III. Predictive Stator Flux and Current Vector Control

The presented predictive control is based on FCS-MPC, which ensures that the stator flux (λ) and current (i_y) follow their reference values. Fig. 2. illustrates an overview of the proposed method. Details will be discussed in the next subsections.

A. Proposed Control System

The continuous-time equations (14) and (15) can be transformed to discrete-time equations using Euler approximation as follows:

$$\lambda(k+1) = \lambda(k) + T_s(u_x(k) - R_s i_x(k)) \quad (18)$$

$$i_y(k+1) = i_y(k) + T_s[-\frac{a}{L_d}(u_x(k) - R_s i_x(k)) + \frac{b}{L_d}(u_y(k) - R_s i_y(k) - w\lambda(k))] \quad (19)$$

Where, T_s is the discretization sampling time and k is the samples number. In the above equations, $\lambda(k)$ will be calculated by the flux observer, which is presented below. Also, the reference currents of the stator flux ($i_{xy}(k)$) can be calculated by the following equations:

$$i_x(k) = i_d(k)\cos\delta(k) + i_q(k)\sin\delta(k) \quad (20)$$

$$i_y(k) = -i_d(k)\sin\delta(k) + i_q(k)\cos\delta(k) \quad (21)$$

Finally, a cost function is exploited to select the optimal switching mode. In the proposed method, the cost function will be based on the predicted flux and current error.

$$G = K\left(\lambda^* - \lambda(k+1)\right)^2 + \left(i_y{}^* - i_y(k+1)\right)^2 \quad (22)$$

The positive coefficient of K is the weight factor of the cost function. The optimal selection of the weigh factor is still a challenge in predictive control [23], [24]. In this paper, the weight factor selection is done with trial and error.

B. Stator Flux Observer

The proposed method requires flux and torque angle observers. An overview of the flux observer is shown in Fig. 3. In this observer, the flux is calculated using the machine voltage equations at the stationary reference frame as follows:

$$u_D = R_s i_D + \frac{d\lambda_D}{dt} \quad (23)$$

$$u_Q = R_s i_Q + \frac{d\lambda_Q}{dt} \quad (24)$$

u_D, u_Q, i_D, i_Q, λ_D, λ_Q are D_Q axis stator voltages, currents and fluxes, respectively.

Using (23) and (24), λ_D and λ_Q can be expressed as:

$$\lambda_D = \int(u_D - R_s i_D + V_{comp})\,dt \quad (25)$$

$$\lambda_Q = \int(u_Q - R_s i_Q + V_{comp})\,dt \quad (26)$$

V_{comp} compensates various errors in flux estimation, such as inverter nonlinearity, dead time, integration dc-offset and stator resistance variation [25].

Flux magnitude can be written as (27).

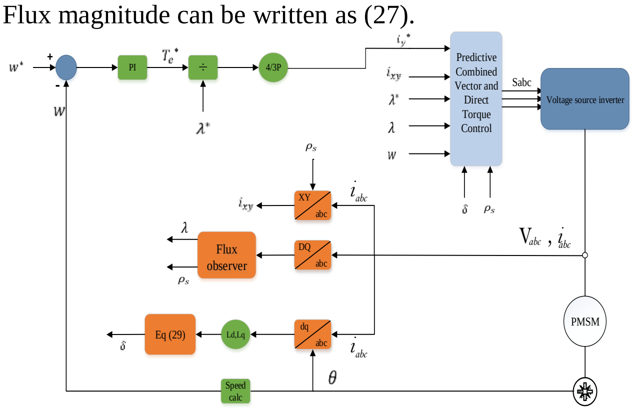

Fig. 2. Block diagram of IPMSM drive system control

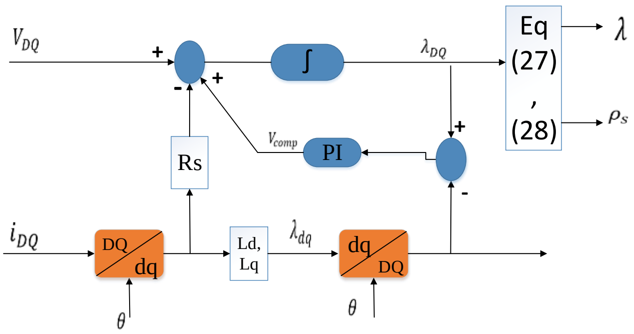

Fig. 3. Stator flux observer

$$\lambda = \sqrt{\lambda_D^2 + \lambda_Q^2} \quad (27)$$

The angle between stator flux axis and machine stationary frame can be attained according to (28) and the torque angle can be obtained from (29).

$$\rho_s = \tan^{-1}(\frac{\lambda_Q}{\lambda_D}) \quad (28)$$

$$\delta = \tan^{-1}(\frac{\lambda_q}{\lambda_d}) \quad (29)$$

IV. Simulation Result

Based on the proposed control strategy introduced in section III, a simulation is performed in MATLAB/Simulink environment. The specifications of the machine are brought in Table I and the block diagram of the control method is presented in Fig. 2. To validate the efficiency of the proposed method, it is compared with the classic DTC and PTC methods. To have a proper comparison, all PI coefficients are set to their optimum values with trial and error, and the average switching frequency of all three methods is set between 4 and 6 kHz. The steady-state performance of the proposed method in comparison to DTC and PTC are shown in Fig. 4 and Fig. 5, respectively. The reference flux, load torque and rotor speed are fixed at 4 Wb, 1 N.m, 800 rpm, respectively. In the predictive method, the time constant (Ts) is assumed to be 100 microseconds.

Clearly, at the steady state condition, the flux and torque variations of the proposed method are less than the other two methods. To be more precise, the torque and stator flux ripples are reduced by 63.6% and 55% in comparison to DTC. These values are 44.4% and 58% for PTC. The reduced variation can help the motor to have smoother performance. Furthermore, the overall efficiency of the system is increased using the suggested control strategy. Having a close look over stator flux of PTC, it can be inferred that the stator flux suffers from

TABLE I. Parameters of the IPMSMs

Parameters	Value	Unit
L_d	42.44	$[mH]$
L_q	79.57	$[mH]$
R_s	2.95	$[\Omega]$
λ_m	.311	$[Wb]$
J (Inertia)	.003	$[Kg.m^2]$
B_m	.0001	$[Nm.\frac{rad}{s}]$
Number of poles	4	--

some spike-shaped currents, which is related to stator flux. These spike-like currents generate unwanted noises. However, these spikes are suppressed in the proposed method to avoid unwanted electromagnetic interference (EMI).

The transient state response of the flux, speed and torque for DTC, PTC and the proposed method are presented in Fig.6 to Fig. 8. Fig. 6, illustrates the responses of all three controllers to the torque step input, where it changes from 1 *N.m* to 3 *N.m*. In this case, the reference values of the stator flux and speed remained constant and merely a torque step is applied to the motor. Although DTC and PTC provide good dynamic responses, the proposed method have relatively smoother transient response.

Fig. 7 presents the response of the control methods to the stator flux reference step input. Again other characteristics kept unchanged (1 *N.m* torque and the same speed of 800 rpm). The results prove the advantage of the proposed method over the two other methods.

In Fig. 8, the transient response of the motor to a speed step input is shown, where speed changes from 800 rpm to 1,300 rpm. The load torque and flux are kept unchanged. The results show that using the proposed method, the motor can reach its ultimate speed faster than the other control methods.

Fig. 9 shows the stator current waveforms for all three different controllers. Contemplating the stator current waveforms in Fig. 9 and the THD values, brought in Fig. 10, it can be inferred that stator current enjoys a more sinusoidal waveform in comparison to the other methods, which results in less mechanical tensions and power loss. To be more precise, THD of the stator current for the proposed method is 3.20% while this value for DTC and PTC are 4.84% and 4.64%, respectively. In other words, the offered method has decreased the current THD by 33.88% in comparison to DTC and 31% in comparison to PTC. It must be mentioned that the current waveforms of three control strategies have been saved in separated simulations, then, current waveforms of different phases (phase A of DTC, phase B of PTC and phase C of the proposed method) are plotted together to have a proper illustration in one figure (see Fig. 9).

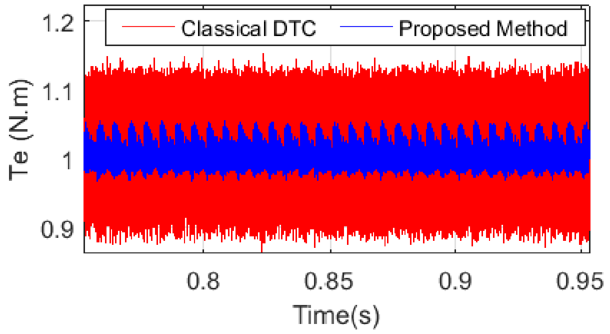

(a)

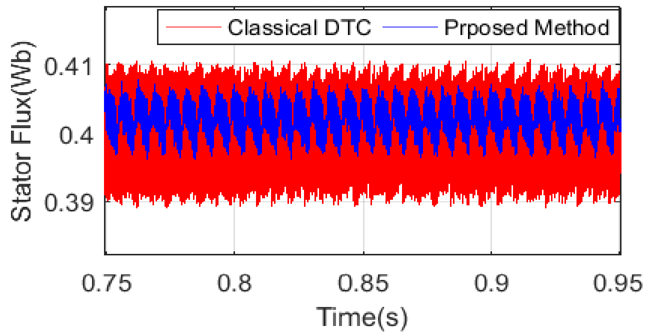

(b)

Fig. 4. Comparison of steady-state response of the proposed method with DTC (a) Electromagnetic Torque (b) Stator Flux

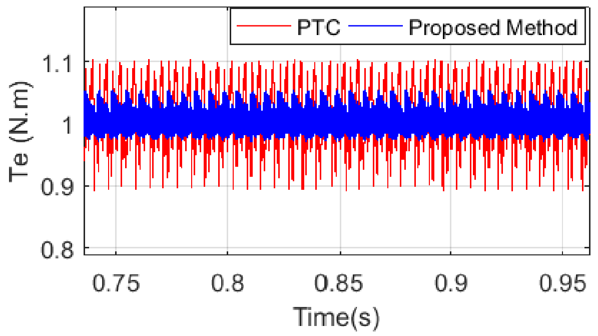

(a)

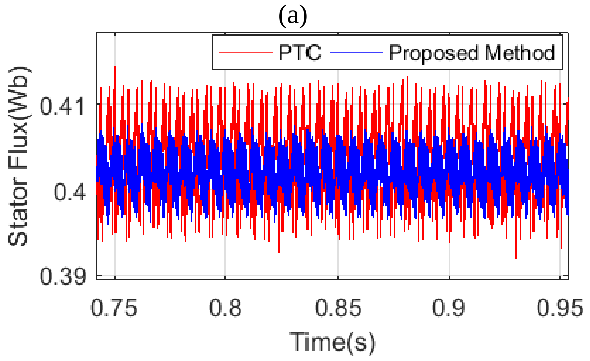

(b)

Fig. 5. Comparison of steady-state response of the proposed method with PTC (a) Electromagnetic Torque (b) Stator Flux

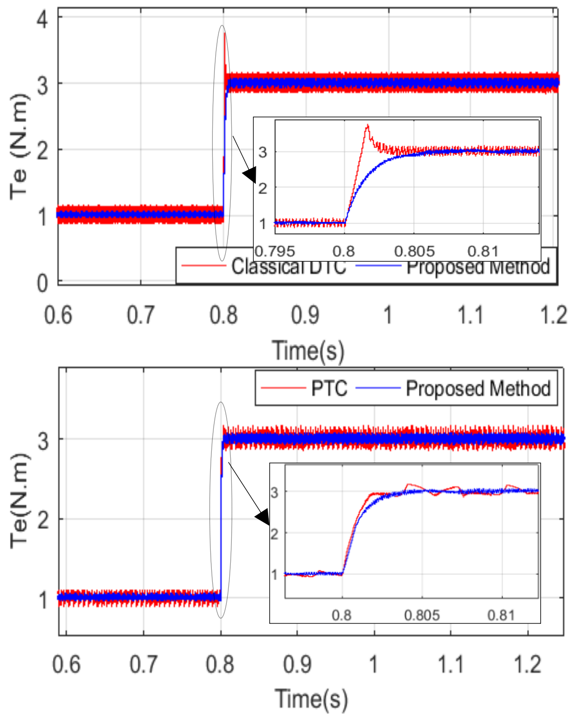

Fig. 6. Comparison of torque transient response of the proposed method with DTC (top) and PTC (bottom)

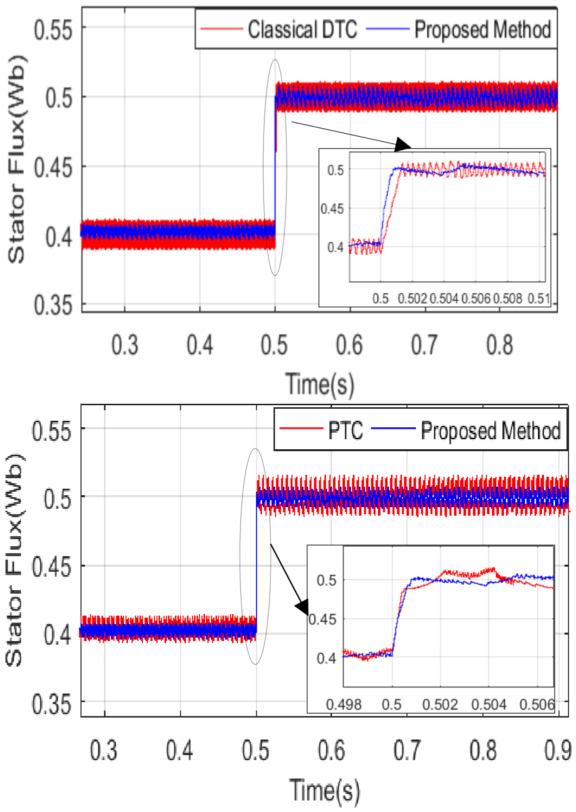

Fig. 7. Comparison of stator flux transint response of the proposed method with DTC (top) and PTC (bottom).

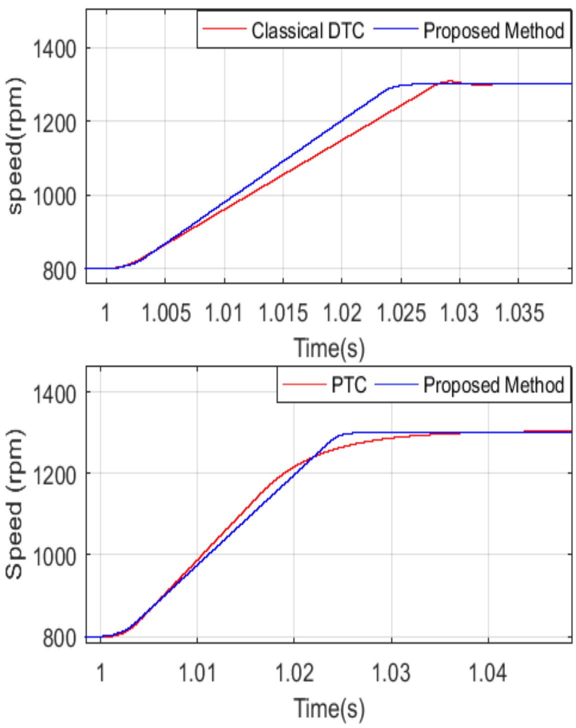

Fig. 8. Comparison of stator speed transint response of the proposed method with DTC (top) and PTC (bottom).

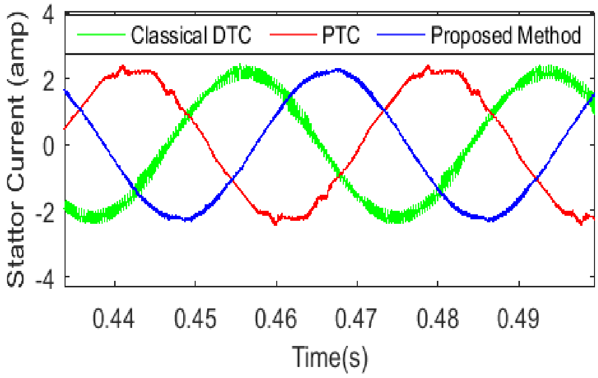

Fig. 9. Comparison of stator current of the proposed method, DTC and PTC.

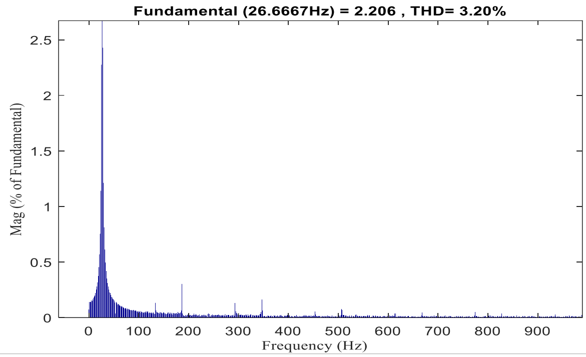

(a)

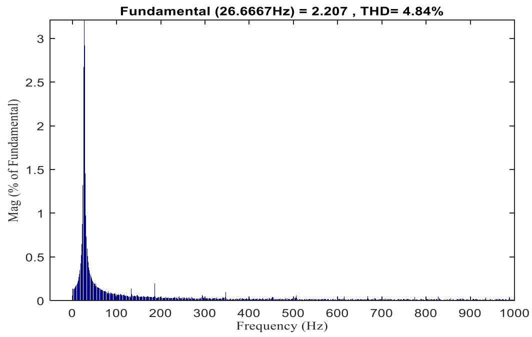

(b)

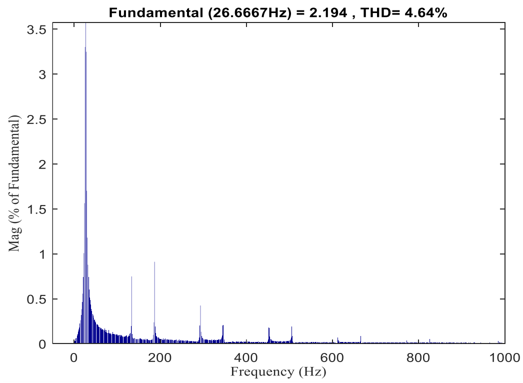

(c)

Fig. 10. Harmonic spectrum of a) the proposed method b) DTC c) PTC

V. CONCLUSION

PMSMs are widely used in various applications. These motors are mainly controlled using DTC and FOC. However, these methods suffer from two major deficiencies: relatively high torque ripple and stator flux ripple. In this regard, in this paper, a new control strategy based on DFVC is suggested to suppress these ripples. A model-predictive control in stator flux frame is employed in which the state variables are the stator flux and y-axis current. Stator flux observer is used to estimate the flux and torque angles. Moreover, a cost function with optimized coefficients are used to optimize the model. To validate the proficiency of the proposed method, a simulation in MATLAB/Simulink is carried out and the results are compared with PTC and DTC. The results illustrate that the proposed control strategy decreases the torque and stator flux ripples by 63.6% and 55% in comparison to DTC. These values are 44.4% and 58% for PTC. Furthermore, the stator current THD enjoys over 30% reduction.

References

[1] M. Moradian, J. Soltani, A. Najjar-Khodabakhsh, and G. R. A. Markadeh, “Adaptive Torque and Flux Control of Sensorless IPMSM Drive in the Stator Flux Field Oriented Reference Frame,” IEEE Trans. Ind. Electron., vol. 63, no. 8, pp. 205–212, 2018.

[2] Z. Mynar, L. Vesely, and P. Vaclavek, “PMSM model predictive control with field-weakening implementation,” International Journal of Recent Advances in Science and Technology, vol. 63, no. 8, pp. 5156–5166, 2016.

[3] A. Sood, and N. Gupta, “Direct torque control scheme of induction motor drive using space vector Modulation.,” IEEE Trans. Ind. Electron., vol. 6, no. 1, pp. 1–7, 2019.

[4] Z. Wang, J. Chen, M. Cheng and K. T. Chau, “Field-Oriented Control and Direct Torque Control for Paralleled VSIs Fed PMSM Drives With Variable Switching Frequencies,” IEEE Trans. Power Electron., vol. 31, no. 3, pp. 2417–2428, 2016.

[5] C. Lascu, A. Argeseanu, and F. Blaabjerg, “Super-Twisting Sliding Mode Direct Torque and Flux Control of Induction Machine Drives,” IEEE Trans. Power Electron., 2019.

[6] S. Vaez-Zadeh and E. Jalali, “Combined vector control and direct torque control method for high performance induction motor drives,” Energy Convers. Manag., vol. 48, no. 12, pp. 3095–3101, 2007.

[7] E. Daryabeigi and S. Vaez-Zadeh, “A combined control for fast and smooth performance of IPM motor drives over wide operating conditions,” IEEE Trans. Energy Convers., vol. 33, no. 3, pp. 1384–1391, 2018.

[8] E. Daryabeigi, A. Mirzaei, H. A. Zarchi, and S. Vaez-Zadeh, “Deviation Model-Based Control of Synchronous Reluctance Motor Drives with Reduced Parameter Dependency,” IEEE Trans. Power Electron., vol. 34, no. 7, pp. 6697–6705, 2018.

[9] H. Karimi, S. Vaez-Zadeh, and F. R. Salmasi, “Combined vector and direct thrust control of linear induction motors with end effect compensation,” IEEE Trans. Energy Convers., vol. 31, no. 1, pp. 196–205, 2015.

[10] J. Mohammadi, S. Vaez-Zadeh, S. Afsharnia, and E. Daryabeigi, “A combined vector and direct power control for DFIG-based wind turbines,” IEEE Trans. Sustain. Energy, vol. 5, no. 3, pp. 767–775, 2014.

[11] S. R. Mohapatra and V. Agarwal, “Model Predictive Controller with Reduced Complexity for Grid Tied Multilevel Inverters,” IEEE Trans. Ind. Electron., 2018.

[12] S. Bayhan, H. Abu-Rub, and R. S. Balog, “Model predictive control of quasi-z-source four-leg inverter,” IEEE Trans. Ind. Electron., vol. 63, no. 7, pp. 4506–4516, 2016.

[13] Y. Zhang,and H. Yang, “Two-Vector-Based Model Predictive Torque Control Without Weighting Factors for Induction Motor Drives,” IEEE Trans. Power Electron., vol. 31, no. 3, pp. 1381–1390, 2016.

[14] S. Rubino, R. Bojoi, S. A. Odhano, and P. Zanchetta, “Model Predictive Direct Flux Vector Control of Multi-three-Phase Induction Motor Drives,” IEEE Trans. Ind. Appl., vol. 54, no. 5, pp. 4394–4404, 2018.

[15] A. Bhowate, M. V Aware, and S. Sharma, “Predictive Torque Control Algorithm for Five-Phase Induction Motor Drive for Reduced Torque Ripple with Switching Frequency Control,” IEEE Trans. Power Electron., 2019.

[16] F. Wang, S. Li, X. Mei, W. Xie, J. Rodríguez, and R. M. Kennel, “Model-based predictive direct control strategies for electrical drives: An experimental evaluation of PTC and PCC methods,” IEEE Trans. Ind. Informatics, vol. 11, no. 3, pp. 671–681, 2015.

[17] M. Siami, D. A. Khaburi, A. Abbaszadeh, and J. Rodríguez, “Robustness improvement of predictive current control using prediction error correction for permanent-magnet synchronous machines,” IEEE Trans. Ind. Electron., vol. 63, no. 6, pp. 3458–3466, 2016.

[18] M. Siami, D. A. Khaburi, and J. Rodriguez, “Torque ripple reduction of predictive torque control for PMSM drives with parameter mismatch,” IEEE Trans. Power Electron., vol. 32, no. 9, pp. 7160–7168, 2016.

[19] Y. Zhang, J. Zhu, and W. Xu, “Predictive torque control of permanent magnet synchronous motor drive with reduced switching frequency,” in 2010 International Conference on Electrical Machines and Systems, pp. 798–803, 2010.

[20] G. Pellegrino, E. Armando, and P. Guglielmi, “Direct-flux vector control of IPM motor drives in the maximum torque per voltage speed range,” IEEE Trans. Ind. Electron., vol. 59, no. 10, pp. 3780–3788, 2011.

[21] H. A. A. Awan, M. Hinkkanen, R. Bojoi, and G. Pellegrino, “Stator-Flux-Oriented Control of Synchronous Motors: Design and Implementation,” in 2018 IEEE Energy Conversion Congress and Exposition (ECCE), pp. 6571–6577, 2018.

[22] H. Hadla and S. Cruz, “Predictive stator flux and load angle control of synchronous reluctance motor drives operating in a wide speed range,” IEEE Trans. Ind. Electron., vol. 64, no. 9, pp. 6950–6959, 2017.

[23] P. G. Ipoum-Ngome, D. L. Mon-Nzongo, J. Song-Manguelle, R. C. C. Flesch, and T. Jin, “Optimal finite state predictive direct torque control without weighting factors for motor drive applications,” IET Power Electron., vol. 12, no. 6, pp. 1434–1444, 2019.

[24] V.P. Muddineni, A.K. Bonala and S.R. Sandepudi, “Enhanced weighting factor selection for predictive torque control of induction motor drive based on VIKOR method,” IET Electric Power Applications. , vol. 10, no. 9, pp. 877–888 2016.

[25] I. Boldea, M. C. Paicu, and G.-D. Andreescu, “Active flux concept for motion-sensorless unified AC drives,” IEEE Trans. Power Electron., vol. 23, no. 5, pp. 2612–2618, 2008.